Symmetry: Culture and Science
Vol. 21, Nos. 1-4, 333-351, 2013

SECTION TITLE

GENERALIZED SELF-CONTACTING SYMMETRIC FRACTAL TREES

Bernat Espigulé Pons

Address: Fortianell n4, 17469 Fortià, Catalunya
E-mail: bernatep@gmail.com. Web: http://pille.iwr.uni-heidelberg.de/~fractaltree01/

Abstract: *The present work identifies and generalizes two different classes of self-contacting binary trees that are separately mapped along the piecewise smooth boundary of the symmetric binary trees Mandelbrot set. The only common tree of these two classes of fractals is the Sierpinski 2-gon gasket tree, commonly known as H-tree, and it is mapped in a topological critical point of the trees Mset boundary. The critical points for other Sierpinski gasket trees (symmetric trees with b equally-spaced branches per node) play an analogous role. Using these critical points as references, we develop a notation to parameterize and classify all the families of generalized symmetric fractal trees. We deduce their boundary equations where the tip-to-tip self-contact takes place, and we provide several diagrams, their fractal dimension and examples of self-contacting fractal trees with N-fold rotational symmetry.*

Keywords: fractal trees, bilateral symmetry, video-feedback, N-fold symmetry.

1. Introduction

One of the most spectacular and accessible phenomena related to the bilateral symmetry is the generation of video-feedback fractal trees in a computer screen. If the screen has a mirror effect enabled, and a webcam starts to record its own output, the system will run into a loop that traps, transforms and copies the recorded frames again and again until they are reduced to mere fixed points forming a fractal attractor. Changing the camera roll angle or the distance to the screen, different fractal patterns emerge. The attractors of this home-made dynamical system are analogous to a family of IFS fractals generated by a pair of affine transforms. Figure 1 compares four video-feedback attractors with their associated symmetric binary fractal trees.

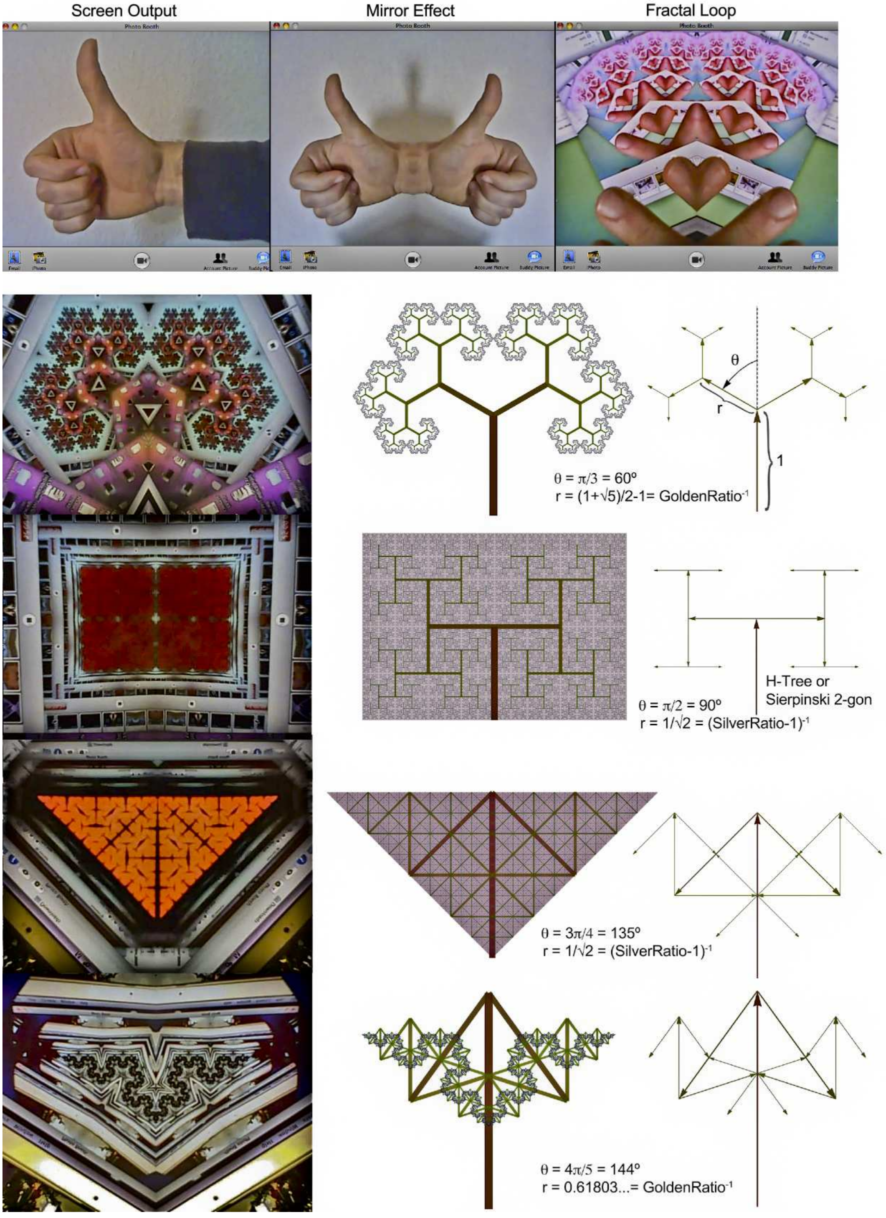

Figure 1: Video-feedback patterns generated using an external webcam, and their fractal trees.

Figure 2 shows the Mandelbrot set for the following family of IFS:

$$\{\mathbb{C};\ w_1(z) = \lambda z + 1,\ w_2(z) = \lambda^* z - 1\}, \quad P = \{\lambda \in \mathbb{C} : |\lambda| < 1\}$$

Where $\lambda^* = (\lambda_1 + i\lambda_2)^* = (\lambda_1 - i\lambda_2)$ is the complex conjugate of λ, the absolute value $|\lambda|$ is the length r of the first pair of branches, and the argument $arg(\lambda)$ is the angle θ between the linear extension of the trunk and the first left branch L. The transformations $w_1(z)$ and $w_2(z)$ are similitudes of scaling factor r, that rotate in opposite directions through the same angle θ.

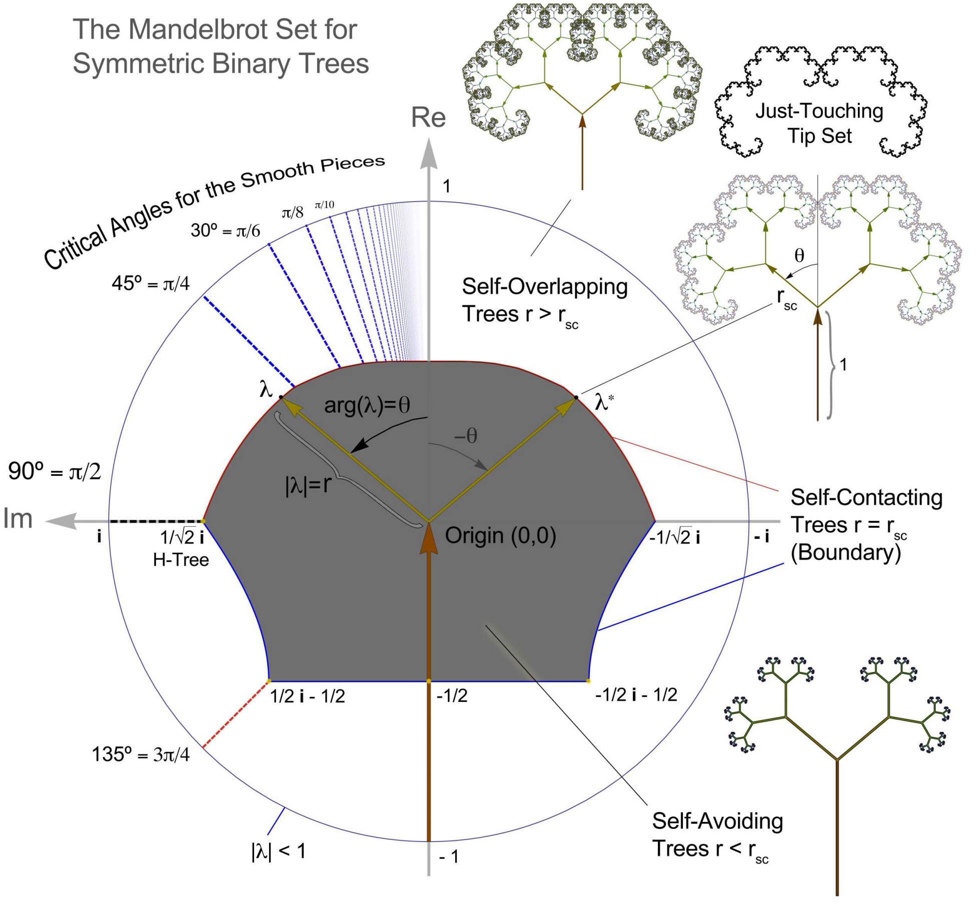

Figure 2: The Mandelbrot Set for Symmetric Binary Trees $T_2(r,\theta)$.

The tree branches are drawn by joining the IFS points generated at each iteration with their corresponding ancestors. Notice that we have set the complex plane's real line $\mathbb{R}$ to be oriented vertically in order to draw the trees looking upwards.

The algebraic curves of this Mandelbrot set boundary were found by Hardin and Barnsley in 1985 [Hardin][Barnsley1988][Barnsley1992]. They proved that this Mandelbrot set is connected, its boundary is the union of a countable set of smooth curves, and is piecewise differentiable. Their work considered solely the attractors of this IFS family, and the associated fractal trees were left behind. Some years after, Mandelbrot and Frame studied self-contacting symmetric binary trees in detail [Mandelbrot], and independently obtained the same union of a countable set of smooth curves that ensures tip-to-tip self-contact for symmetric binary trees. They didn't related these trees to the earlier work of Hardin and Barnsley, but, as it is shown in [Wolfram], both approaches are equivalent and should be presented in a unified way.

Figures 2 and 3 indicate different aspects of the piecewise smooth Mandelbrot set. The dark region of the Mandelbrot set is were all the self-avoiding trees are mapped. Their tip set or attractor is disconnected forming thus a Cantor set in the complex plane with dimension $D = log(2)/log(1/r)$. For $r \leqslant 1/2$ the trees are always self-avoiding, regardless of the value of θ. However, for $1/2 < r < 1$, the tree may or may not be self-avoiding, depending on θ.

When the value r starts to increase the tip set starts to condensate until it reaches a critical value r_{sc} where the tip set becomes connected. All the trees that have the top of its first pair of branches, L and R, placed in the map's boundary are self-contacting binary fractal trees $T_2(r_{sc}, \theta)$. Outside the critical boundary $r > r_{sc}(\theta)$ all the trees are self-overlapping and they inevitably contain branch-crossing.

The bilateral mirror symmetry around the linear extension of the trunk enables us to label all the branches with addresses that are finite sequences of letters L and R. Therefore the branches are denumerable but the branch tips are not as they are defined by an infinite sequence, see Figure 4. When the infinite address of a tip is eventually periodic, closed expressions for the coordinates can be found by summing the appropriate geometric series. A symmetric binary tree depends only on two parameters: the angle θ between the branch L and the linear extension of the trunk E, and the scaling ratio $r < 1$ which is also the length of the L and R pair of branches.

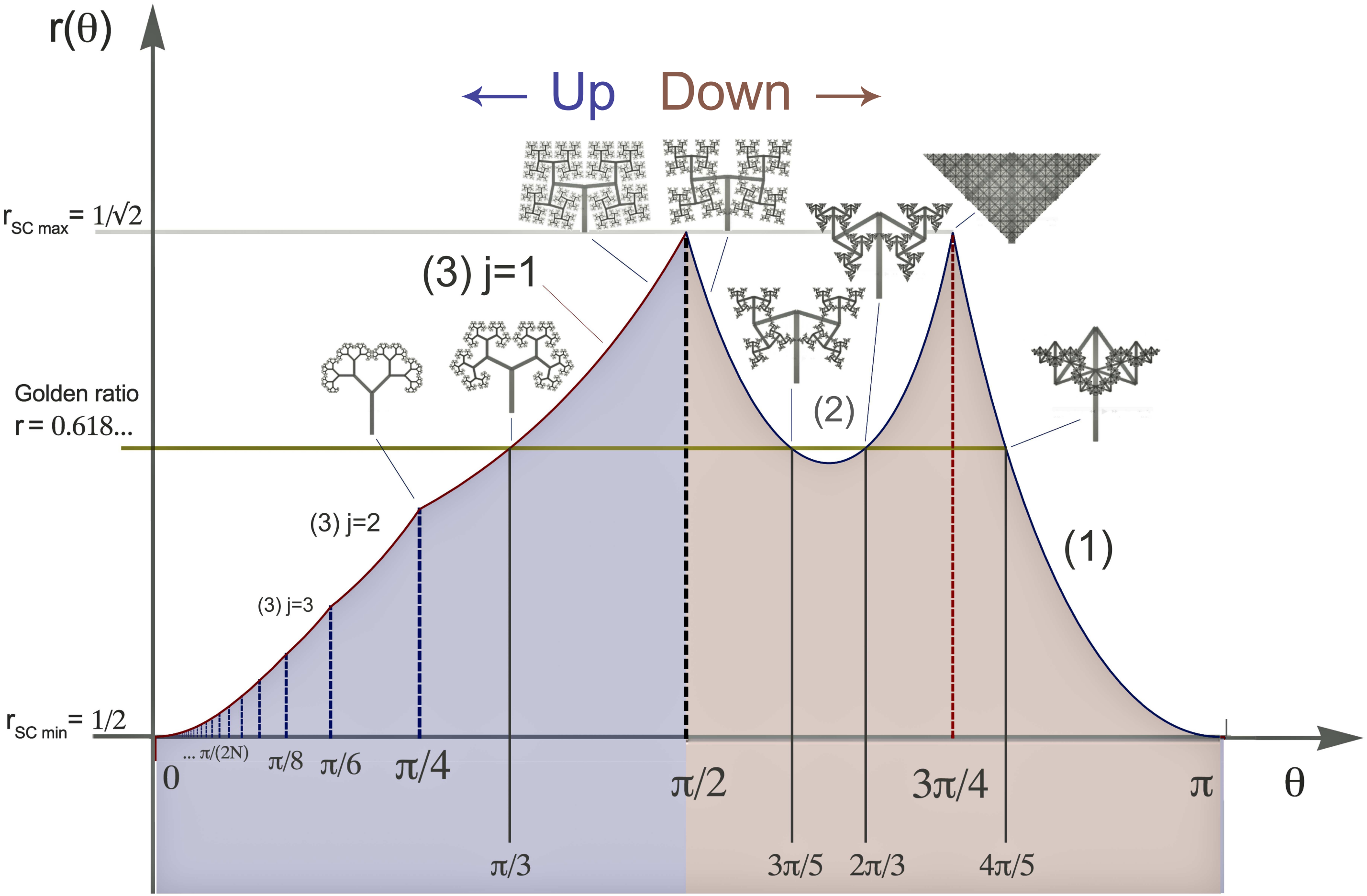

Figure 3: Cartesian map of the Mandelbrot set for Symmetric Binary Trees $T_2(r, \theta)$.

The origin $(0,0)$ of our coordinate system is placed at the top of the canonical trunk of length 1. The turning angles associated to the address letters L and R in symmetric binary trees $T_2(r,\theta)$ are $L \to (\theta)$ and $R \to (-\theta)$. For example, the coordinates (x,y) of the branch LR are found to be:
$(r^1 sin\theta + r^2 sin(\theta + (-\theta)), r^1 cos\theta + r^2 cos(\theta + (-\theta)) = (r sin\theta, r cos\theta + r^2)$.

Therefore, the coordinates of tips with periodic sequences can be easily computed, for example, the tip L^∞ has coordinates (x,y):

$$(r sin\theta + r^2 sin(2\theta) + ..., r cos\theta + r^2 cos(2\theta) + ...) = \left(\frac{r\sin(\theta)}{r^2-2r\cos(\theta)+1}, -\frac{r(r-\cos(\theta))}{r^2-2r\cos(\theta)+1}\right).$$

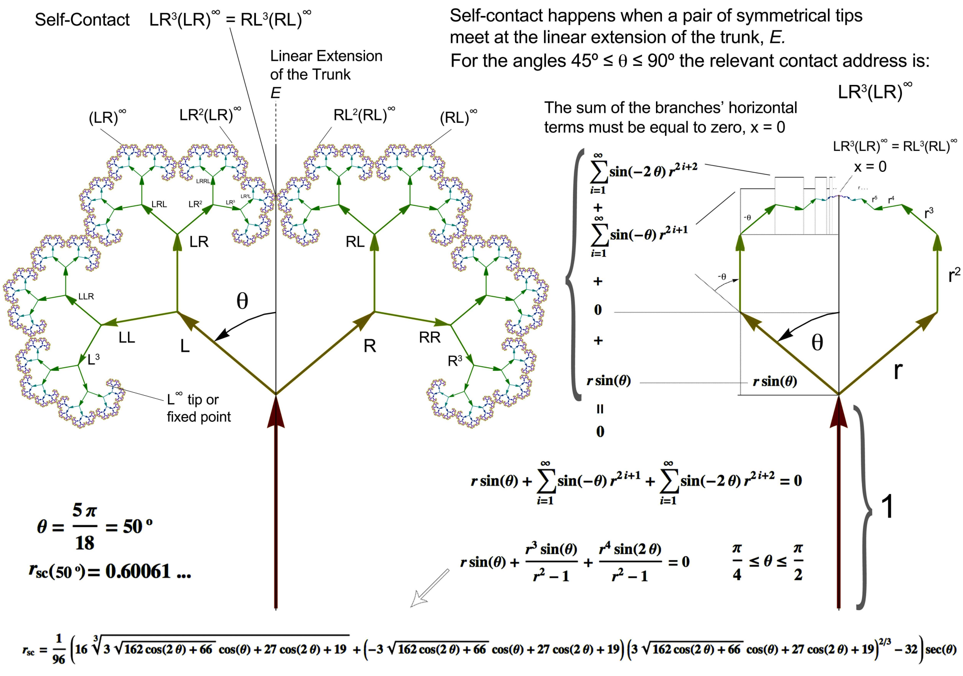

Figure 4: A Self-Contacting Symmetric Binary Tree with relevant address $LR^3(LR)^\infty$.

Figure 4 shows how the self-contacting equation $r_{sc}(\theta)$ is deduced from the tip address $LR^3(LR)^\infty$ with the condition that its tip must lie in the linear extension of the trunk, i.e. its horizontal coordinate must be zero, $x = 0$. Therefore, careful observations of the relevant self-contacting tip addresses for different intervals of θ can be used to deduce all the equations that ensure self-contact, $r_{sc}(\theta)$.

For $\frac{3\pi}{4} \leq \theta \leq \pi$, the relevant branch tip is $L(LR)^\infty$ which provides the following expression:
$r\sin(+\theta) + \sum_{i=1}^{\infty} \sin(\theta+\theta) r^{2i} + \sum_{i=1}^{\infty} \sin(\theta-\theta+\theta) r^{2i+1} = 0$
which can be reduced to $r\sin(\theta) - \frac{r^2\sin(2\theta)}{r^2-1} - \frac{r^3\sin(\theta)}{r^2-1} = 0$, and solved for r:

$$r_{sc} = -\frac{1}{2\cos(\theta)} \tag{1}$$

For the interval $\frac{\pi}{2} \leq \theta \leq \frac{3\pi}{4}$, the relevant tip address is $L^2(LR)^\infty$ and its related equation is:

$$r_{sc} = \frac{2\sin(\theta)}{8\sqrt{\sin^6(\theta)\cos^2(\theta)} - \sin(4\theta)} \tag{2}$$

For $0 < \theta \leq \dfrac{\pi}{2}$, there is an infinite countable set of smooth pieces, and the desired branch tips are given by the addresses $LR^{j+2}(LR)^\infty$ for the intervals $\frac{\pi}{2j+2} \leq \theta \leq \frac{\pi}{2j}$ and j values ranging from 1 to ∞. The implicit equations deduced from this kind of addresses are given by:

$$\frac{r^2\left(r^{j+1}(-\cos(\theta(j+1))) + r^{j+2}\cos(\theta j) - r\cos(\theta) + 1\right)}{r^2 - 2r\cos(\theta) + 1} = \frac{1}{2} \tag{3}$$

The critical angle $\theta = \dfrac{\pi}{2}$ divides the trees in two main classes, the Up binary trees ($\theta < \dfrac{\pi}{2}$), with a tip set connected above the trunk, and the Down binary trees ($\theta > \dfrac{\pi}{2}$), with a tip set intersecting the trunk. The diagram of Figure 3 shows a Cartesian map, r versus θ, of the binary trees Mandelbrot set, the secondary critical trees ($T_2(r_{sc}, \pi/4)$ and $T_2(r_{sc}, 3\pi/4)$), two different class trees close to the H-tree, and the four self-contacting symmetric binary trees that scale with the golden ratio. The interesting properties of these four golden trees where first noted and described by Tara Taylor [Taylor 2005][Taylor 2007].

2. Generalized Up and Down Symmetric Fractal Trees

The H-tree, $\theta = \dfrac{\pi}{2}$, that separates the two main classes of symmetric binary trees can be generalized to mirror-symmetric trees with b equally-spaced branches per node and $\theta = \dfrac{\pi}{b}$, see Figure 6. These trees play an analogous role for symmetric trees with $b > 2$ branches per node. Thus, generalized symmetric fractal trees are also divided in two different classes: the Up symmetric fractal trees with their tip set connected above the trunk, and the Down symmetric fractal trees with their tip set intersecting the trunk, see Figures 5,7,8 and 10.

Any generalized symmetric tree can be characterized using three parameters: the angle θ between the linear extension of the trunk and the branch L_1, the length $r < 1$ of this branch, and the number of branches b with length r. They are denoted by $DT_b(r, \theta)$ or $UT_b(r, \theta)$ depending on its class, down or up respectively. Again, the bilateral mirror symmetry around the linear extension of the trunk enables us to label all the branches with addresses that are finite sequences of letters. The n left branch is L_n, the down branch is D, the up branch is U and the n right branch is R_n. Like in symmetric binary trees, when the infinite address of a tip is eventually periodic, closed expressions for its coordinates can be found by summing the appropriate geometric series. The fact that they also posses well-defined critical angles, and a countable set of relevant addresses, allows us to deduce the generalized self-contacting boundary equations for all the families of symmetric fractal trees.

3. Tip-to-Tip Self-Contact for Down Symmetric Trees

For down symmetric fractal trees $DT_b(r, \theta)$ the branch angle turns are:

$L_n \to (\theta + (n-1)\alpha)$
$R_n \to (-\theta - (n-1)\alpha)$
$D \to 0$

where the angle α between secondary branches is given by $\alpha = \dfrac{2(\pi - \theta)}{b-1}$.

Self-contact occurs when a tip can be accessed by different branch addresses without crossings, for example, the addresses $L_2L_1(L_1R_1)^\infty$ and $R_2R_1(R_1L_1)^\infty$ in Figure 5 represent the same tip.

Note that, for DT_b with even number of branches b, the self-similarity and left-right symmetry of the tree imply that self-avoidance is guaranteed if none of the branch descendants of the first left branch $L_{b/2}$ intersects the trunk. Tip-to-tip self-contact occurs where the rightmost branch tip of the left half of the tree meets the trunk. Again, the scaling ratio that ensures self-contact r_{sc} depends on the

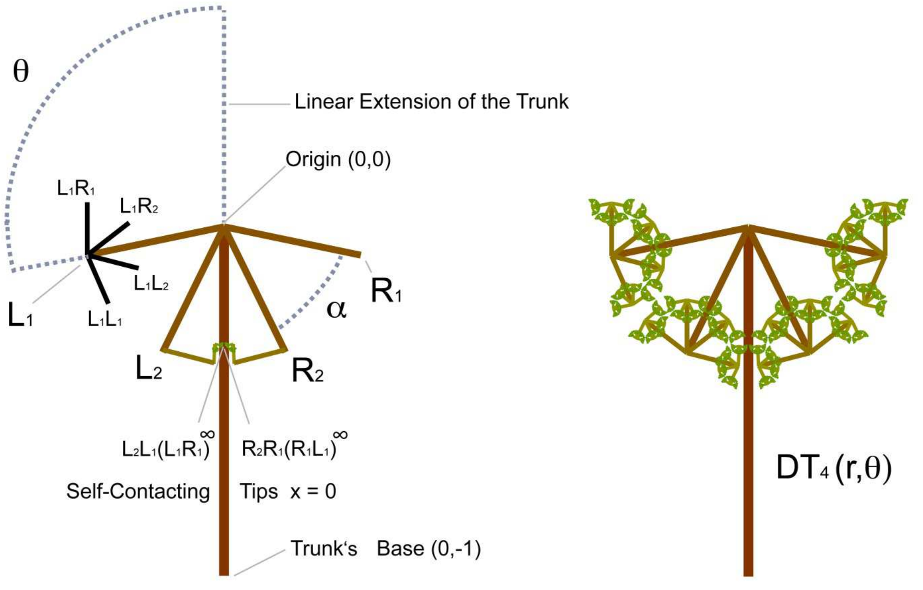

Figure 5: First branch addresses for Down Symmetric Fractal Trees with even b.

angle θ and the number of branches b.

For $\frac{(b+1)\pi}{2b} \leq \theta \leq \pi$ the relevant address is $L_{b/2}(L_1 R_1)^\infty$; that is, after the initial $L_{b/2}$ branch, the branches alternate bearing left L_1 and right R_1. Combining all like terms, we see that the branch tip lies on E if its x coordinate is 0; that is, if:

$$r \sin\left(\frac{\left(\frac{b}{2}-1\right)(2(\pi-\theta))}{b-1} + \theta\right)$$
$$+ \sum_{i=1}^{\infty} r^{2i} \sin\left(\frac{\left(\frac{b}{2}-1\right)(2(\pi-\theta))}{b-1} + 2\theta\right)$$
$$+ \sum_{i=1}^{\infty} r^{2i+1} \sin\left(\frac{\left(\frac{b}{2}-1\right)(2(\pi-\theta))}{b-1} + \theta\right) = 0;$$

This expression can be reduced and solved explicitly for r:

$$\frac{r\left(\sin\left(\frac{\pi-\theta}{b-1}\right) + r\sin\left(\frac{\pi-b\theta}{b-1}\right)\right)}{r^2-1} = 0 \quad \longrightarrow \quad r_{sc} = -\sin\left(\frac{\pi-\theta}{b-1}\right)\csc\left(\frac{\pi-b\theta}{b-1}\right) \quad (4)$$

Figure 6 shows the families of boundary equations which determine the length r_{sc} of the L_1 branch as function of the angle θ. The red smooth pieces in the interval $\frac{(b+1)\pi}{2b} \leq \theta \leq \pi$ represent the family of self-contacting trees given by (4). The tip set of these trees form generalized von Koch curves different from the commonly encountered in the literature [Keleti]. They have interesting properties related the diagonals of regular polygons, and their tip set remains connected as a 3D fractal curves when their branches are being unfolded [Espigule 2013A].

For $\frac{\pi}{b} \leq \theta < \frac{(b+1)\pi}{2b}$, there are two kinds of relevant addresses, $L_{b/2}L_n(R_1L_1)^\infty$ and $L_{b/2}L_n(L_1R_1)^\infty$, which alternate each other for every n at well defined critical angles; starting with the addresses $L_{b/2}L_1(R_1L_1)^\infty$ at the angles $\frac{(b+1)\pi}{2b}$ and ending at $\theta = \frac{\pi}{b}$ when the letter L_n becomes $L_{(2+b)/4}$ or $L_{(4+b)/4}$ depending on b.

For the angle intervals $\frac{\pi(b-4n+3)}{2(b-2n+1)} \leq \theta < \frac{\pi(b-4n+5)}{2(b-2n+2)}$ the relevant addresses are $L_{b/2}L_n(R_1L_1)^\infty$. The subindex n takes all the integer values from 1 to $(2+b)/4$. Here, again a closed expression for r can be deduced:

$$\begin{aligned}
&r\sin\left(\frac{\left(\frac{b}{2}-1\right)(2(\pi-\theta))}{b-1}+\theta\right)\\
&+r^2\sin\left(\frac{\left(\frac{b}{2}-1\right)(2(\pi-\theta))}{b-1}+\theta+\frac{(2(\pi-\theta))(n-1)}{b-1}+\theta\right)\\
&+\sum_{i=2}^{\infty} r^{2i-1}\sin\left(\frac{\left(\frac{b}{2}-1\right)(2(\pi-\theta))}{b-1}+\theta+\frac{(2(\pi-\theta))(n-1)}{b-1}+\theta-\theta\right)\\
&+\sum_{i=2}^{\infty} r^{2i}\sin\left(\frac{\left(\frac{b}{2}-1\right)(2(\pi-\theta))}{b-1}+\theta+\frac{(2(\pi-\theta))(n-1)}{b-1}+\theta-\theta+\theta\right)=0
\end{aligned}$$

this can be reduced to the following implicit equation:

$$\frac{r\left(r\left(\sin\left(\frac{\theta(b-2n+2)+\pi(2n-3)}{b-1}\right)+r\sin\left(\frac{(\pi-\theta)(2n-3)}{b-1}\right)\right)+\left(r^2-1\right)\sin\left(\frac{\pi-\theta}{b-1}\right)\right)}{r^2-1}=0$$

which can be solved for r to obtain the following closed form:

$$r=\frac{2\sin\left(\frac{\pi-\theta}{b-1}\right)}{\sqrt{\sin^2\left(\frac{\pi(3-2n)-\theta(b-2n+2)}{b-1}\right)+4\sin\left(\frac{\pi-\theta}{b-1}\right)\left(\sin\left(\frac{\pi-\theta}{b-1}\right)+\sin\left(\frac{(\pi-\theta)(2n-3)}{b-1}+2\theta\right)\right)}+\sin\left(\frac{\theta(b-2n+2)+\pi(2n-3)}{b-1}\right)} \tag{5}$$

The plots for this families of equations (5) are represented in blue, see Figure 6.

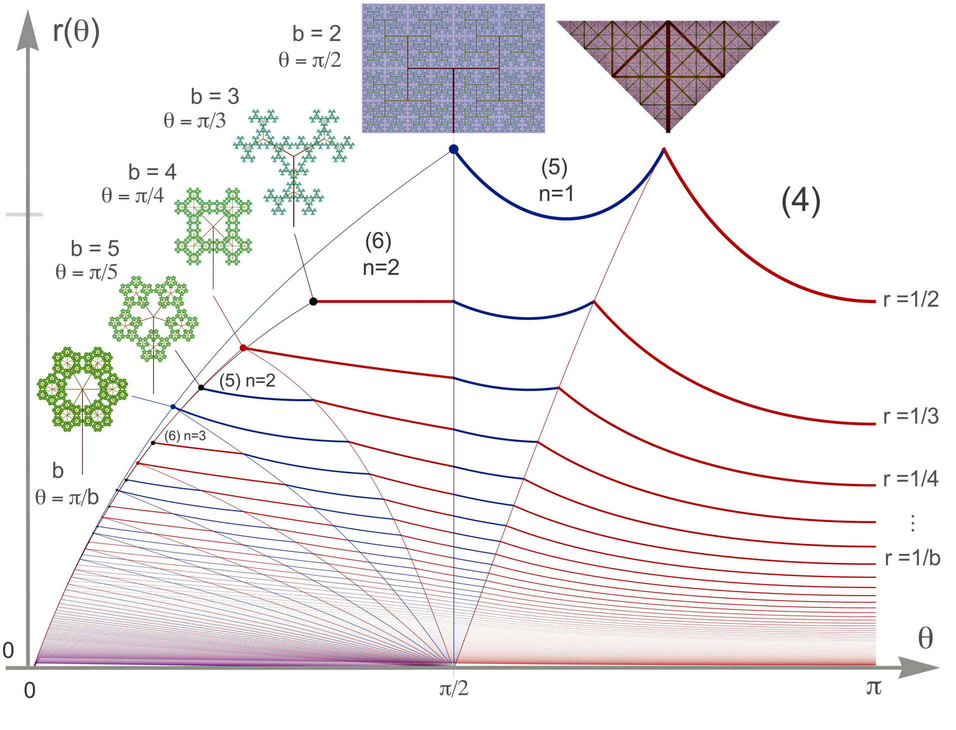

Figure 6: Self-Contact Curves $r_{sc}(\theta)$ for Generalized Down Symmetric Trees.

For the angle intervals $\frac{\pi(b-4n+5)}{2(b-2n+2)} \leq \theta < \frac{\pi(b-4n+7)}{2(b-2n+3)}$ the relevant addresses are $L_{b/2}L_n(L_1R_1)^\infty$. The subindex n takes the integer values from 2 to $(4+b)/4$. An analogous calculation to the other kind of addresses can be carried out as follow:

$$r\sin\left(\frac{\left(\frac{b}{2}-1\right)(2(\pi-\theta))}{b-1}+\theta\right)$$
$$+r^2\sin\left(\frac{\left(\frac{b}{2}-1\right)(2(\pi-\theta))}{b-1}+\frac{(2(\pi-\theta))(n-1)}{b-1}+\theta+\theta\right)$$
$$+\sum_{i=2}^{\infty}r^{2i-1}\sin\left(\frac{\left(\frac{b}{2}-1\right)(2(\pi-\theta))}{b-1}+\frac{(2(\pi-\theta))(n-1)}{b-1}+\theta+\theta+\theta\right)$$
$$+\sum_{i=2}^{\infty}r^{2i}\sin\left(\frac{\left(\frac{b}{2}-1\right)(2(\pi-\theta))}{b-1}+\frac{(2(\pi-\theta))(n-1)}{b-1}+\theta+\theta+\theta-\theta\right)=0$$

reducing it we obtain the following families of implicit equations:

$$\frac{r\left(r\left(\sin\left(\frac{\theta(b-2n+2)+\pi(2n-3)}{b-1}\right)+r\sin\left(\frac{2b\theta+\theta-2\theta n+2\pi n-3\pi}{b-1}\right)\right)+\left(r^2-1\right)\sin\left(\frac{\pi-\theta}{b-1}\right)\right)}{r^2-1}=0$$

which can be solved explicitly for r:

$$r_{sc}=\frac{\sqrt{\sin^2\left(\frac{\pi(3-2n)-\theta(b-2n+2)}{b-1}\right)+4\sin\left(\frac{\pi-\theta}{b-1}\right)\left(\sin\left(\frac{\pi-\theta}{b-1}\right)+\sin\left(\frac{(\pi-\theta)(2n-3)}{b-1}\right)\right)}+\sin\left(\frac{\pi(3-2n)-\theta(b-2n+2)}{b-1}\right)}{2\left(\sin\left(\frac{\pi-\theta}{b-1}\right)+\sin\left(\frac{(\pi-\theta)(2n-3)}{b-1}\right)\right)} \tag{6}$$

This families of equations (6) are represented in red, and they are grouped in families of values $n = 2, 3, ..., \infty$. The first family $n = 2$ starts at $\theta = \frac{\pi}{2}$.

The three types of general equations deduced for down trees with even b are also valid for trees with odd number of b branches per node. It is an easy exercise to show that down symmetric fractal trees with odd b, see Figure 7, have tip-to-tip conditions that provide the same families of equations (4), (5) and (6). The smooth curves represented in Figure 6 parameterize the families of self-contacting down symmetric fractal trees, $DT_b(r_{sc}, \theta)$.

4. Tip-to-Tip Self-Contact for Up Symmetric Trees

The turning angles associated to the address letters L_n, R_n and U in up symmetric fractal trees $UT_b(r, \theta)$ are:

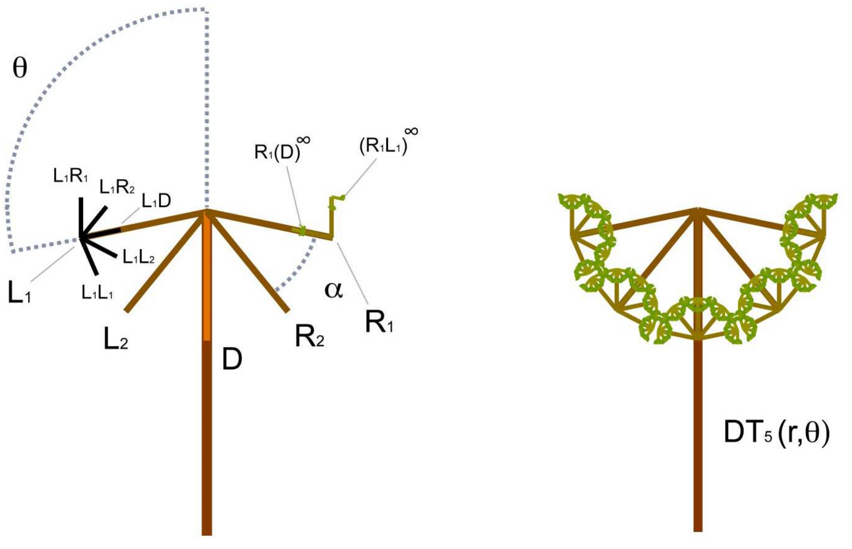

Figure 7: First branch addresses for Down Symmetric Fractal Trees with odd b.

$L_n \to (\theta - (n-1)\alpha)$
$R_n \to (-\theta + (n-1)\alpha)$
$U \to 0$

The term α is the angle between neighboring branches and it is given by $\alpha = \dfrac{2\theta}{b-1}$.

For UT_b with even number of branches b, see Figure 8, the self-similarity and left-right symmetry of the tree imply that self-avoidance is guaranteed if none of the descendant branches of the first left branch $L_{b/2}$ intersects the linear extension E of the trunk. Tip-to-tip self-contact occurs where the rightmost branch tip of the left half of the tree lies on E.

For the angle intervals $\frac{\pi}{2} \leq \theta \leq \frac{\pi(b-1)}{b}$, there are two kinds of relevant addresses when b is even.

The first kind of addresses has the form $L_{\frac{b}{2}} R_n \left(R_{\frac{b}{2}} L_{\frac{b}{2}}\right)^\infty$. They take place in the intervals $\frac{\pi(b-1)}{2(b-2n+1)} \leq \theta \leq \frac{\pi(b-1)}{2(b-2n)}$ from $n = 1$ to $n = \dfrac{b}{4}$. And when the condition $x = 0$ is imposed, their families of self-contacting equations are:

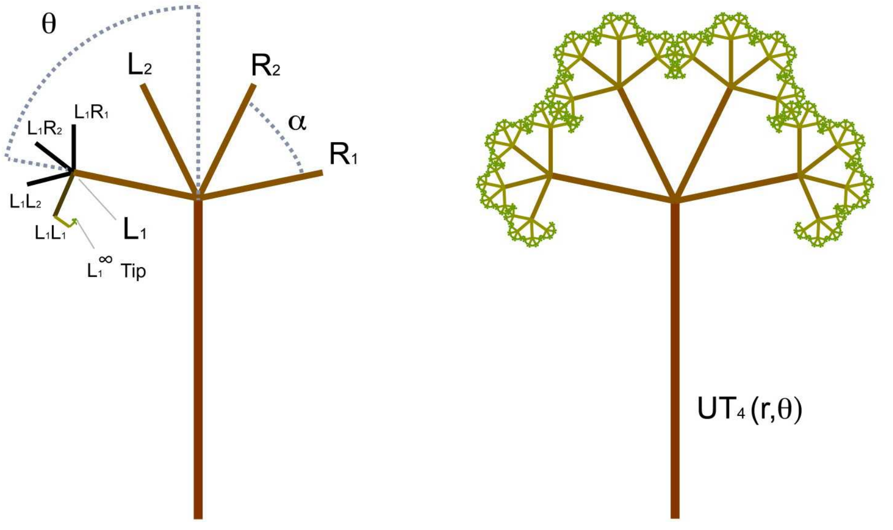

Figure 8: First branch addresses for Up Symmetric Fractal Trees with even b.

$$r_{sc} = \frac{\sqrt{\sin^2\left(\frac{\theta(b-2n)}{b-1}\right) - 4\sin\left(\frac{\theta}{1-b}\right)\left(\sin\left(\frac{\theta}{b-1}\right) + \sin\left(\frac{\theta(b-2n+1)}{b-1}\right)\right)} - \sin\left(\frac{\theta(b-2n)}{b-1}\right)}{2\left(\sin\left(\frac{\theta}{b-1}\right) + \sin\left(\frac{\theta(b-2n+1)}{b-1}\right)\right)} \tag{7}$$

The second kind of addresses has the form $L_{\frac{b}{2}} R_n \left(L_{\frac{b}{2}} R_{\frac{b}{2}}\right)^{\infty}$, which take place in the intervals $\frac{\pi(b-1)}{2(b-2n)} \leq \theta \leq \frac{\pi(b-1)}{2(b-2n-1)}$ from $n = 1$ to $n = \dfrac{b-2}{4}$. Their families of self-contacting equations is given by:

$$r_{sc} = \frac{\sqrt{\sin^2\left(\frac{\theta(b-2n)}{b-1}\right) - 4\sin\left(\frac{\theta}{1-b}\right)\left(\sin\left(\frac{\theta}{b-1}\right) + \sin\left(\frac{\theta(b-2n-1)}{b-1}\right)\right)} - \sin\left(\frac{\theta(b-2n)}{b-1}\right)}{2\left(\sin\left(\frac{\theta}{b-1}\right) + \sin\left(\frac{\theta(b-2n-1)}{b-1}\right)\right)} \tag{8}$$

Figure 9 shows the smooth curves for generalized up symmetric fractal trees. The equations (7) are represented in red, and the equations (8) are colored in blue.

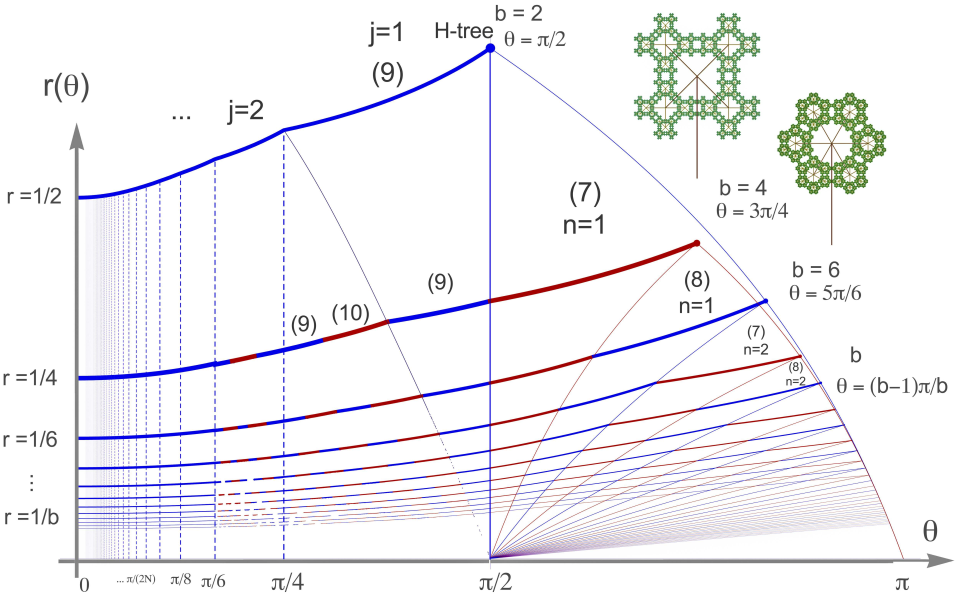

Figure 9: Self-Contact Curves $r_{sc}(\theta)$ for Generalized Up Symmetric Trees with even b.

For the remaining interval $0 < \theta \leq \frac{\pi}{2}$, the boundary curves are partitioned in a rather complicated way. Additionally to the critical angles $\frac{\pi}{4}, \frac{\pi}{6}, \frac{\pi}{8}, \ldots$ found in up binary trees, see Figure 2, when the number of branches b gets bigger and bigger, more and more secondary critical angles start to appear in-between. Nonetheless the two kinds of relevant addresses can be presented in the following forms:

$$L_{\frac{b}{2}} \left(R_1\right)^j R_{\frac{b}{2}-n} \left(L_{\frac{b}{2}} R_{\frac{b}{2}}\right)^\infty$$

for the intervals $\frac{\pi(b-1)}{2(b-1)j+4n+2} \leq \theta \leq \frac{\pi(b-1)}{2(b-1)j+4n}$, where the index j takes the values from 1 to ∞, and for each j, n takes the values from $n = 0$ to $n = \frac{b}{2} - 1$.

and

$$L_{\frac{b}{2}} \left(R_1\right)^j R_{\frac{b}{2}-n} \left(L_{\frac{b}{2}} R_{\frac{b}{2}}\right)^\infty$$

for the intervals $\frac{\pi(b-1)}{2(b-1)j+4n} \leq \theta \leq \frac{\pi(b-1)}{2(b-1)j+4n-2}$ where the index j takes the values from 1 to ∞, and for each j, n takes the values from $n = 1$ to $n = \frac{b}{2} - 1$.

The first kind of addresses provides the following families of implicit equations:

$$\frac{r^{j+2}\left(\sin\left(\frac{\theta((b-1)j+2n)}{b-1}\right)+r\sin\left(\frac{\theta((b-1)j+2n+1)}{b-1}\right)\right)}{r^2-1}+\frac{r^{j+2}\sin\left(\theta\left(\frac{1}{1-b}+j+1\right)\right)}{r^2-2r\cos(\theta)+1}$$
$$+\frac{r^{j+3}\sin\left(\theta\left(\frac{1}{b-1}-j\right)\right)}{r^2-2r\cos(\theta)+1}-\frac{r^2\sin\left(\frac{(b-2)\theta}{b-1}\right)}{r^2-2r\cos(\theta)+1}+\frac{r\sin\left(\frac{\theta}{1-b}\right)(2r\cos(\theta)-1)}{r^2-2r\cos(\theta)+1}=0 \tag{9}$$

And the second kind of addresses leads to the following families of implicit equations:

$$\frac{r^{j+2}\sin\left(\frac{\theta((b-1)j+2n)}{b-1}\right)}{r^2-1}+\frac{r^{j+3}\sin\left(\frac{\theta((b-1)j+2n-1)}{b-1}\right)}{r^2-1}+\frac{r^{j+2}\sin\left(\frac{\theta((b-1)j+b-2)}{b-1}\right)}{r^2-2r\cos(\theta)+1}$$
$$-\frac{r^{j+3}\sin\left(\frac{\theta((b-1)j-1)}{b-1}\right)}{r^2-2r\cos(\theta)+1}+\frac{r\left(r\sin\left(\frac{b\theta}{1-b}\right)-\sin\left(\frac{\theta}{1-b}\right)\right)}{r^2-2r\cos(\theta)+1}=0 \tag{10}$$

The smooth pieces defined by (9) and (10) are represented in blue and red respectively, see Figure 9.

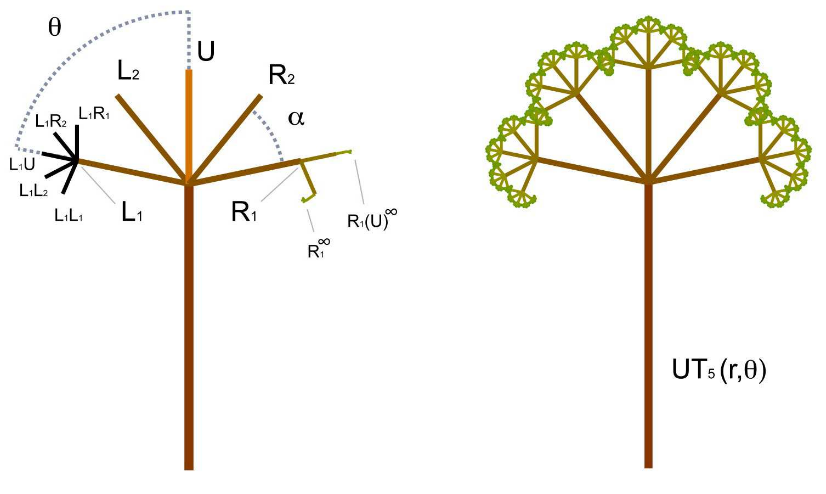

Figure 10: First branch addresses for Up Symmetric Fractal Trees with odd b.

For UT_b with odd number of branches b, see Figure 10, the relevant self-contact pair of tips lies outside the linear extension of the trunk. The condition imposed here is that the self-contacting tips must have the same coordinates, or simply that their vertical coordinates must be equal, $y = y$.

For the intervals $\frac{\pi}{2} \leq \theta \leq \frac{\pi(b-1)}{b}$, the relevant tip pairs have the following form:

$\mathrm{UL}_n(U)^\infty = L_{\frac{b-1}{2}} R_n(U)^\infty$ in the intervals $\frac{\pi(b-1)}{2(b-2n+1)} \leq \theta \leq \frac{\pi-\pi b}{-2b+4n+2}$ for every n with values from $n = 0$ to $n = \frac{b-3}{2}$. Imposing the condition $y = y$ the following family of self-contacting equations is deduced explicitly for r_{sc}:

$$r_{sc} = \frac{1}{1 - \csc\left(\frac{\theta}{1-b}\right)\sin\left(\frac{\theta(b-2n)}{b-1}\right)} \tag{11}$$

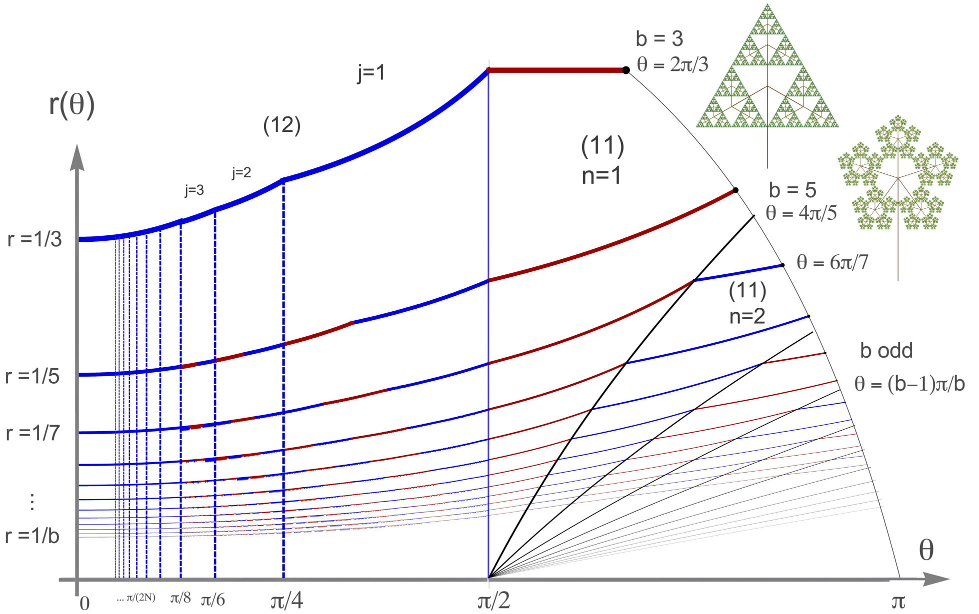

Figure 11: Self-Contact Curves $r_{sc}(\theta)$ for Generalized Up Symmetric Trees with odd b.

For the remaining interval $0 < \theta \leq \frac{\pi}{2}$, the boundary curves are partitioned in a similar way for this found for b even. This time, there is only one kind of implicit equations, and it is deduced from the following family of relevant tip pairs:

$L_{\frac{b-1}{2}} (R_1)^j (R_{\frac{b-1}{2}-n})^\infty = \mathrm{UL}_1 (L_1)^j L_{\frac{b-1}{2}-n}(U)^\infty$, which are valid for the intervals $\frac{\pi(b-1)}{2(b-1)j-4n+4} \leq \theta \leq \frac{\pi(b-1)}{2(b-1)j-4n}$, with values n from 0 to $\frac{b-3}{2}$ and j from 1 to ∞.

Summing up the appropriate vertical terms for both tips, we obtain the following families of implicit equations:

$$\frac{r^{j+2}\left(\sin\left(\frac{\theta((b-1)j+2n)}{b-1}\right)+\sin\left(\frac{\theta((b-1)j+2(n+1))}{b-1}\right)\right)}{r-1}+\frac{r^{j+2}\left(\sin\left(\frac{\theta((b-1)j+b-3)}{b-1}\right)+\sin(\theta(j+1))\right)}{r^2-2r\cos(\theta)+1}$$
$$+\frac{r^{j+3}\left(\sin\left(\frac{\theta(-bj+j+2)}{b-1}\right)-\sin(\theta j)\right)}{r^2-2r\cos(\theta)+1}-\frac{r^2\left(\sin\left(\frac{(b-3)\theta}{b-1}\right)+r\sin\left(\frac{2\theta}{b-1}\right)+\sin(\theta)\right)}{r^2-2r\cos(\theta)+1}+r\sin\left(\frac{2\theta}{b-1}\right)=0 \tag{12}$$

The boundary curves for $UT_b(r,\theta)$ with odd number of branches b are represented in Figure 11.

5. Fractal Dimension for Generalized Symmetric Trees

When $UT_b(r,\theta)$ or $DT_b(r,\theta)$ have no double point, it is said to be *self-avoiding*. If so, the branch tips are distinct points and, like the points in a Cantor set, are non-denumerable. Their tip set form a self-similar fractal of dimension $D = log(b)/log(1/r)$. For $r < 1/b$, $UT_b(r,\theta)$ and $DT_b(r,\theta)$ are always self-avoiding regardless of the value of θ. However, for $1/b < r < 1$, the tree may or may not be self-avoiding, depending on θ. The dimension of the tip set for a self-contacting tree is given by $D = log(b)/log(1/r_{sc})$.

6. Final Remarks

The broader class of symmetric fractal trees and their self-contacting equations presented here, generalize and extent the previous works of Mandelbrot, Frame, Pagon, and Taylor on the special case of self-contacting symmetric binary fractal trees [Mandelbrot][Pagon][Taylor2005][Taylor2007]. Furthermore, the down self-contacting trees given by eq.(4) and represented in Figure 6, were found to be associated to an interesting type of self-contacting symmetric fractal trees that provide a new generalization to the von Koch curves [Espigule 2013A]. For more examples and further details about fractal trees, the reader is encouraged to visit the author's website dedicated to fractal trees, with fully detailed maps, galleries, animations and interactive *Mathematica's CDF documents*, as well as an extensive annotated bibliography [Espigule 2013B].

Acknowledgements

The author thanks Susanne Krömker for her enthusiastic support of the author's research during an Erasmus exchange at Heidelberg Universität. Susanne's past research on fractals at her *Visualization and Numerical Geometry Group* inspired the author in many different ways. The initial research for this paper was partially done under the inestimable help of Jofre Espigulé, author's twin brother, and it was enriched with many constructive comments of several professors and friends including Warren Dicks, Gaspar Orriols and Carlos Castro.

REFERENCES

Barnsley, M. (1988) *Fractals everywhere*. San Diego: Academic Press, Inc.

Barnsley, M.F. and Hardin, D.P. (1989) A Mandelbrot set whose boundary is piecewise smooth. *Transactions of the American Mathematical Society*, 315, no. 2, 641-658.

Espigulé Pons, B. (2013) Unfolding Symmetric Fractal Trees. In Hart, G. ed. To appear in *Proceedings of the 2013 Bridges Conference on Mathematical Connections in Art, Music, and Science*.

Espigulé Pons, B. (2013) Fractal Trees Project, http://pille.iwr.uni-heidelberg.de/~fractaltree01

Hardin, D.P. (1985) *Hyperbolic iterated function systems and applications*. [Ph.D. Dissertation], Atlanta: Georgia Institute of Technology, 87 pp.

Keleti, T. and Paquette, E. (2010) The Trouble with von Koch Curves Built from n-gons. *The American Mathematical Monthly*, JSTOR, 117, no. 2, 124-137.

Mandelbrot, B.B. and Frame, M. (1999) The Canopy and Shortest Path in a Self-Contacting Fractal Tree. *The Mathematical Intelligencer*, Springer, 21, no. 2, 18-27.

Pagon, D (2003) Self-Similar Planar Fractals Based on Branching Trees and Bushes. *Progress of Theoretical Physics Supplement*, no. 150, 176-187.

Taylor, T.D (2005) *Computational Topology and Fractal Trees*. [Ph.D. Dissertation], Halifax, Nova Scotia.

Taylor, T.D. (2007) Golden Fractal Trees. In: Sarhangi, R. and Barallo, J., eds. *Proceedings of the 2007 Bridges Conference on Mathematical Connections in Art, Music, and Science*, 181-188.

Wolfram, S. (2002) *A New Kind of Science*. Section 8.6, [http://www.wolframscience.com/nksonline/section-8.6], 1st ed., Wolfram Media.